NANO-MICRO LETTERS

Vol. 2, No.4
277-284 (2010)

Enhanced Photoelectrochemical Properties of Cu_2O-loaded Short TiO_2 Nanotube Array Electrode Prepared by Sonoelectrochemical Deposition

Yanbiao Liu, Haibin Zhou, Jinhua Li, Hongchong Chen, Di Li, Baoxue Zhou* and Weimin Cai

Copper and titanium remain relatively plentiful in earth crust. Therefore, using them in solar energy conversion technologies are of significant interest. In this work, cuprous oxide (Cu2O)-modified short TiO2 nanotube array electrode was prepared based on the following two design ideas: first, the short titania nanotubes obtained from sonoelectrochemical anodization possess excellent charge separation and transportation properties as well as desirable mechanical stability; second, the sonoelectrochemical deposition technique favours the improvement in the combination between Cu2O and TiO2 nanotubes, and favours the dispersion of Cu2O particles. UV-Vis absorption and photo- electronchemical measurements proved that the Cu2O coating extended the visible spectrum absorption and the solar spectrum-induced photocurrent response. Under AM1.5 irradiation, the photocurrent density of the composite electrode (i.e. sonoelectrochemical deposition for 5 min) was more than 4.75 times as high as the pure nanotube electrode. Comparing the photoactivity of the Cu2O/TiO2 electrode obtained using sonoelectrochemical deposition with others that synthesized using plain electrochemical deposition, the photocurrent density of the former electrode was ~2.2 times higher than that of the latter when biased at 1.0 V (vs. Ag/AgCl). The reproducible photocurrent response under intermittent illumination demonstrated the excellent stability of the composite electrode. Such kind of composite electrode material will have many potential applications in solar cell and other fields.

Keywords: Cu_2O; Short TiO_2 nanotube array; Sonoelectrochemical deposition

Citation: Yanbiao Liu, Haibin Zhou, Jinhua Li, Hongchong Chen, Di Li, Baoxue Zhou and Weimin Cai, "Enhanced Photoelectrochemical Properties of Cu_2O-loaded Short TiO_2 Nanotube Array Electrode Prepared by Sonoelectrochemical Deposition", Nano-Micro Lett. 2, 277-284 (2010). doi:10.3786/nml.v2i4.p277-284

Fujishima and Honda first demonstrated in 1972 that water could be electrolyzed by irradiating an n-type TiO_2 photoanode with solar energy and hydrogen could be produced at the photocathode in an electrochemical cell [1]. This fascinating discovery initiated lots of investigations in search of more efficient semiconductor materials for photoelectrochemical applications. Among the available photosensitive semiconductor materials, TiO_2 considered as one of the most promising photocatalysts due to its special features, such as low cost, chemical inertness and photostability [2]. However, its wide band gap (3.0~3.2 eV) allows it to absorb only ultraviolet light which accounts for merely ~5% of the solar photons, thereby hampering its wide use. Therefore, considerable attempts aimed at improving the visible light absorption of TiO_2 have been taken [3-5]. Among them, sensitization of TiO_2 with narrow bandgap semiconductors, including CdS, CdSe, Fe_2O_3, SnO_2, etc, has been reported recently to reveal promising reactivity under visible light illumination [6-8].

Cuprous oxide (Cu_2O) is a semiconductor having a direct band gap of 2.0 eV, which has been studied previously for application in solar energy converting devices [9]. A major attraction of Cu_2O is that it is an inexpensive, non-toxic and readily available material. However, semiconductor materials with band gap suitable for capturing a significant fraction of incident solar

School of Environmental Science and Engineering, Shanghai Jiao Tong University, No. 800 Dongchuan Rd., Shanghai, China
*Corresponding author. E-mail: zhoubaoxue@sjtu.edu.cn

spectrum energy (≈0.8~2.4 eV) typically suffer UV induced photocorrosion [10]. It has been reported that the stability of Cu_2O were greatly altered by the material it was coupled with. For instance, Cu_2O coupled with ZnO was reported to be unstable [11], while Cu_2O/TiO_2 junctions are relatively stable [12, 13]. Therefore, the applications of the visible-light- responsive Cu_2O/TiO_2 composite electrode into photoelectron- chemical fields have become a hot subject [10, 14]. Since the conduction band of Cu_2O is ca. ~1.0 eV more negative than that of TiO_2, the coupling of the semiconductors should have a beneficial role in improving charge separation and transfer, as given in Fig. 1. Excited electrons from Cu_2O can be quickly transported to TiO_2, arriving at the electron collectors from external circuit [14]. Factors affecting the photoelectrochemical reactivity of Cu_2O/TiO_2 electrode include the transfer and recombination of photo-generated charges as well as the incident light absorption, which is further determined by the morpho-logical structure of Cu_2O and TiO_2 as well as their combination effectiveness. Therefore, two aspects, including TiO_2 and Cu_2O, can be taken into consideration.

From the view point of TiO_2, the highly ordered TiO_2 nanotube array (TNA) obtained from the anodization of titanium in HF or [F^-]-based electrolyte can reduce the scattering of free electrons and enhance electron mobility [15], which offers the potential for improved electron transport leading to higher photocatalytic efficiency. Therefore, the coupled Cu_2O/TNA photoanode might facilitate kinetic separation of photogenerated charges and decrease the recombination rate within the electrode materials [16, 17]. However, the structural parameters (i.e. tube length and tube diameter) of the TNA film directly influence the transport resistance of photogenerated electrons and the recombination rate among photogenerated charges as well as the practical engineering application of electrode materials. Literatures [18, 19] have also demonstrated that the increase in length of nanotubes may not contribute positively to the photoelectrochemical performance of electrode materials. Recently, a short TNA (referred as STNA) film electrode prepared via sonoelectrochemical anodization route (anodization under irradiation of ultrasonic wave) was reported by our group [20]. Compared with the long nanotubes synthesized by conventional magnetic agitation technique [15, 21], the STNA electrode shows excellent charge separation and transfer properties and desirable mechanical stability.

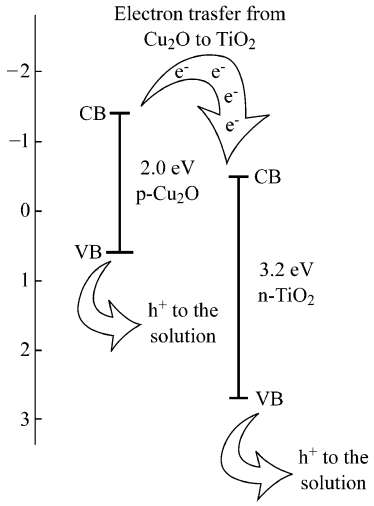

FIG. 1. Schematic diagram illustrating the energy band position and the electron transfer direction for Cu_2O/TiO_2 composite electrode after being excited by light. CB and VB refer to the energy levels of the conduction and valence bands, respectively, of Cu_2O and TiO_2.

As for Cu_2O, the combination of Cu_2O with nanotube layer and the morphological structure of Cu_2O were significantly affected by the Cu_2O preparation pathways. To date, Cu_2O can be fabricated by many different techniques including thermal, anodic and chemical oxidation as well as reactive sputtering [22]. Among these different synthesis techniques, the electrochemical deposition technique offers the simplest and most controllable way of synthesizing Cu_2O/TNA electrodes [23]. However, obtaining a composite electrode with better quality, evenly distributed Cu_2O particles and a strong combination of Cu_2O and TiO_2 nanotubes may be more useful if ultrasonic waves can be integrated into the electrochemical process, since the sonochemical process can help increase the mass transfer throughout the reaction system and accelerate the diffusion of [Cu^+] ions onto the nanotubes.

Based on the above design ideas and our previous work [19-21, 24-26], an efficient photoelectrochemical photoanode (Cu_2O-decorated STNA) was prepared via sonoelectrochemical anodization and sonoelectrochemical deposition (SED, electrochemical deposition under ultrasonic wave irradiation) methods in this work. To our best knowledge, no study has been reported to date regarding the application of SED technique into fabrication of Cu_2O/TiO_2 composite electrode. In our research, the detailed synthesis process, characterization, and photo- electrochemical property testing for this composite catalyst were also discussed.

Experiments

Materials

Titanium sheets (0.25 mm thick, 99.9% purity) were supplied by Sumitomo Chemical (Japan). Hydrofluoric acid (HF, ≥40 wt%), ethanol, acetone, sodium sulfate, sodium acetate and cupric acetate were purchased from Sinopharm Chemical Rea-

gent Company without further treatment prior to use. All solutions were prepared using high-purity deionized (DI) water.

Preparation of STNA

The detailed methodology of the preparation of short, robust and highly-ordered titania nanotube array have been published in our previous work (see Fig. S1 in Supplementary Information) [20]. The anodized samples were then rinsed with DI water and dried in air. Subsequently, the as-prepared STNA samples were crystallized by annealing in air atmosphere for 3 h at 450℃ with heating and cooling rate of 1℃/min.

Cu_2O sonoelectrochemical deposition

The Cu_2O/STNA was synthesized by the sonoelectrochemical deposition method (SED) in a solution contained 0.1 M sodium acetate and 0.02 M cupric acetate at -0.25 V for 5 min at room temperature. In all cases, the electrolyte was freshly prepared. After the deposition, the samples were immediately removed from the electrolyte and sequentially rinsed with DI water. The prepared Cu_2O/STNA electrodes were then annealed at 200℃ for 60 min in nitrogen atmosphere. In order to examine the effect of ultrasonic waves, the Cu_2O-decorated STNA were prepared by plain electrochemical deposition (PED) under the same conditions without sonication treatment.

Characterization

The surface morphology of the samples was characterized with a field emission scanning electron microscope (PHILIPS, Netherlands, Sirion200) equipped with an energy dispersive X-ray spectroscopy (OXFORD, U.K.). An X-ray diffractometer (BRUKER, AXS-8, and ADVANCE) was used to determine the crystalline structure of the samples. The composition of the samples was analyzed with an X-ray photoelectron spectroscopy (Kratos, Axis Ultra DLD, Al Kα radiation). Light absorption properties of the electrode materials were measured using a UV-Vis diffuse reflectance spectrum (TU-1901, Beijing Purkinje General Instrument Co., Ltd).

Apparatus and methods

The photoelectrochemical experiments were performed in a rectangular shaped quartz reactor (20×40×50 mm) using a three-electrode system with a platinum foil counter electrode, a saturated Ag/AgCl reference electrode and a TiO_2 work electrode. The supply bias and work current were controlled using a CHI electrochemical analyzer (CHI 660C, CH Instruments, Inc., USA). The photocurrent was measured at a scan rate of 20 $mV \cdot s^{-1}$ with 0.1 M Na_2SO_4 solution as the electrolyte. A 350 w Xe lamp (Shanghai Lansheng Electronic Co., Ltd) was used as the simulated solar light. For the visible light irradiation, the white light was passed through an optical filter (Nantong Zhenhua co., Ltd), which cut off wavelength below 400 nm.

Results and discussion

Figure 2(a) presents a typical field emission scanning electron microscope (FE-SEM) image of the titania nanotube array obtained by sonoelectrochemical anodization of titanium in HF-H_2O electrolyte, which reveals a regularly arranged pore structure of the film. These pores possess a uniform distribution ~65 nm in diameter and ~280 nm in length. Details on the formation mechanism of the nanotubes synthesized by sonoelectrochemical anodization were described elsewhere [20]. A light green colored deposit is observed on the nanotube surface within 1 min and only a few octahedral Cu_2O particles are deposited (see Fig. 2(b)). As the deposition time increases, the size of Cu_2O particles and their surface coverage increases and the color of the surface also changes from light green to reddish-violet. After 5 min, the nanotube surface becomes extensively coated with a relatively uniform layer of octahedral Cu_2O deposits having side length of ~400 nm and some particles are inserted into the tubular structures (see Fig. 2(c)). For further deposition, the Cu_2O layer clearly covers nearly the entire nanotubular surface (see Fig. 2(d)). Figure 2(e) presents the FE-SEM image of typical Cu_2O-loaded STNA fabricated by plain electrochemical deposition (PED) method for 5 min. Compared with the samples prepared with SED for 5 min (see Fig. 2(c)), the Cu_2O deposits with different size are unevenly distributed throughout the nanotube surface when applying the PED method. This indicates that the SED technique is helpful in obtaining a more uniform distribution of Cu_2O particles on the STNA surface. The success of the preparation of Cu_2O-loaded STNA is further confirmed by the elemental dispersive X-ray (EDX) spectrum. The characteristic peaks in the spectrum are associated with Ti, O, and Cu, and the atomic ratio of Cu element is ~5.21% for the Cu_2O/STNA sample with Cu_2O SED for 5 min (see Fig. 2(f)).

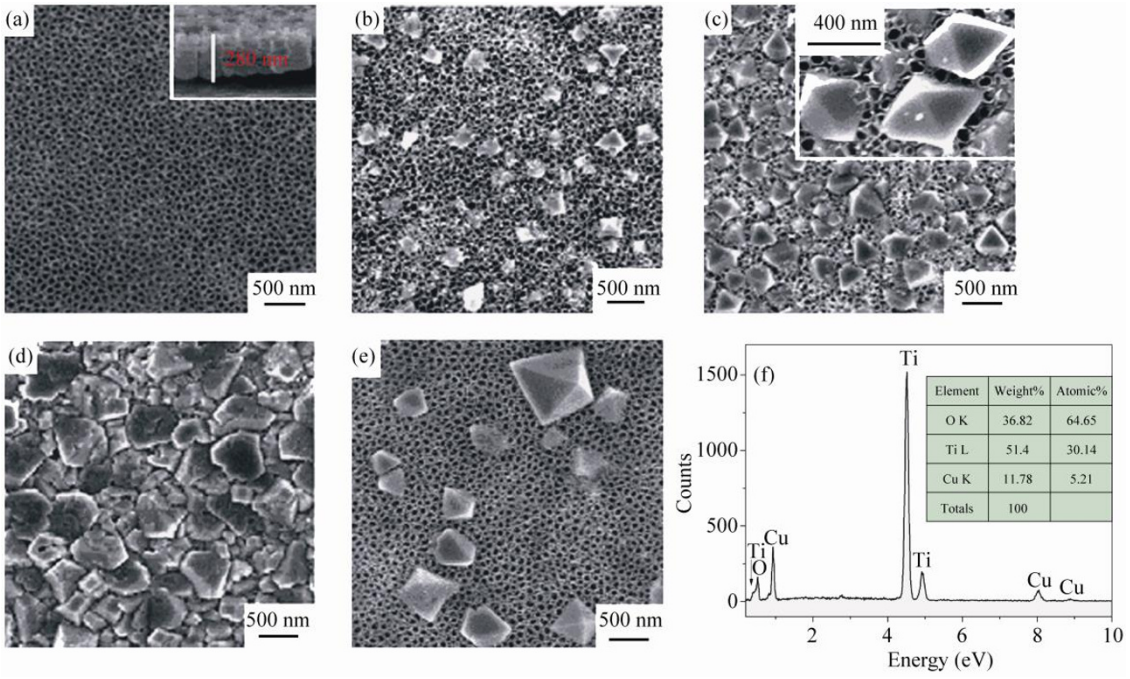

FIG. 2. FE-SEM images of the STNA electrode before: (a); after Cu_2O sonoelectrochemical deposition for different periods: (b) 1 min, (c) 5 min, and (d) 10 min;. (e) STNA electrode after Cu_2O plain electrochemical deposition for 5 min; (f) EDX spectrum of the Cu_2O/STNA sample shown in Figure 2(c).

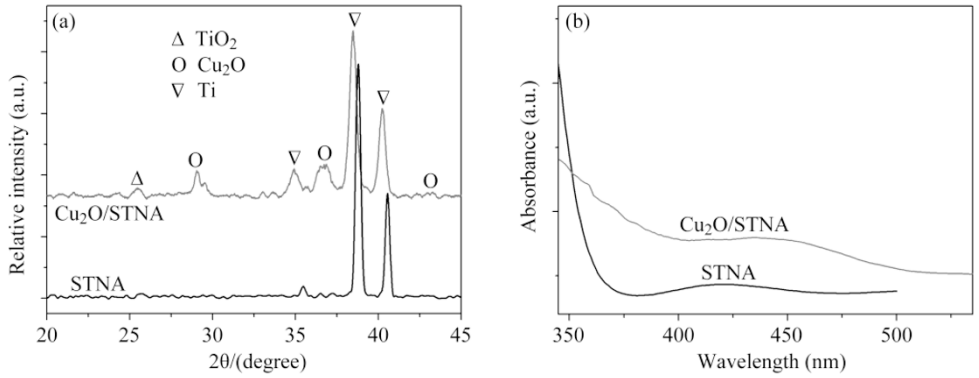

FIG. 3. (a) XRD and (b) UV-vis absorption spectra of Cu_2O/STNA (SED time of Cu_2O is 5 min) and pure STNA.

Figure 3(a) compares the X-ray diffraction (XRD) patterns of a typical as-annealed STNA sample taken before and after Cu_2O SED process at -0.25 V for 5 min. As can be seen that the STNA sample without Cu_2O deposition exhibits strong characteristic peaks of titanium substrate and weak characteristic peak of anatase TiO_2 (this can be attributed to the short tube length of the nanotube layer, ~280 nm). While the Cu_2O-loaded sample shows clearly the crystalline phase of Cu_2O. Furthermore, the characteristic peaks of Cu and CuO are not found, which also testifies to the superiority of this method with regard to electrode purity. The UV-Vis absorption spectra of plain TiO_2 nanotubes and sonoelectrochemically prepared Cu_2O/STNA electrode (deposition time of Cu_2O is 5 min) are given in Fig. 3(b). It is evident that the pure STNA electrode has no obvious absorption of visible light. However, the spectrum of Cu_2O/STNA shows evident absorption in both the UV and visible region, indicating the Cu_2O deposits can be used to sensitize the TiO_2 nanotubes for longer wavelength region of sunlight and the enhanced ability of the Cu_2O/STNA electrode to absorb visible light makes it a promising photocatalyst for solar-driven applications.

Figure 4(a) gives the general scan spectrum of the X-ray photoelectron spectroscopy (XPS) over a large energy range at low resolution of a Cu_2O/STNA electrode where the SED time of Cu_2O is 5 min, showing the presence of Ti, O, Cu and C. Figure 4(b) shows the Cu 2p core level XPS scans, at higher resolution over smaller energy windows. As can be seen, the Cu 2p core level XPS spectrum has two sharp peaks at 932.3 eV (Cu $2p_{3/2}$) and 952.2 eV (Cu $2p_{1/2}$), which is in good agreement with the reported values for Cu_2O [14, 27].

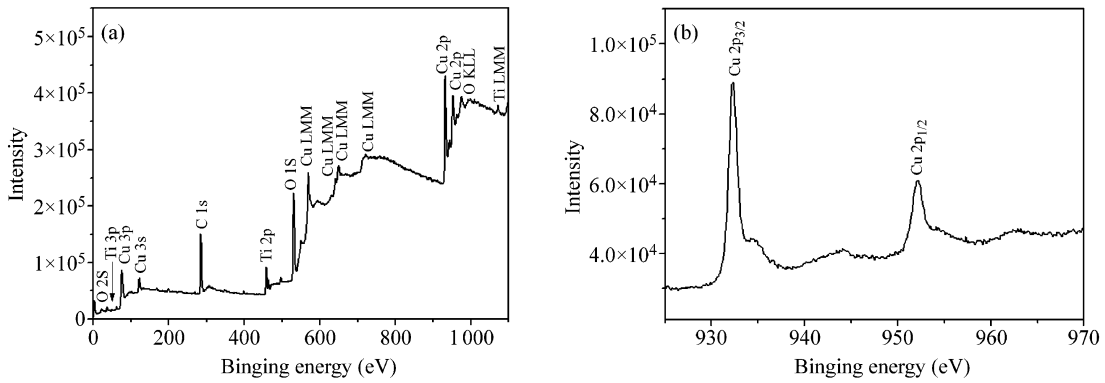

FIG. 4. (a) XPS survey scan for Cu_2O/STNA electrode over a large range at low resolution; (b) Cu 2p XPS core level spectra of Cu_2O/STNA electrode (SED time of Cu_2O is 5 min).

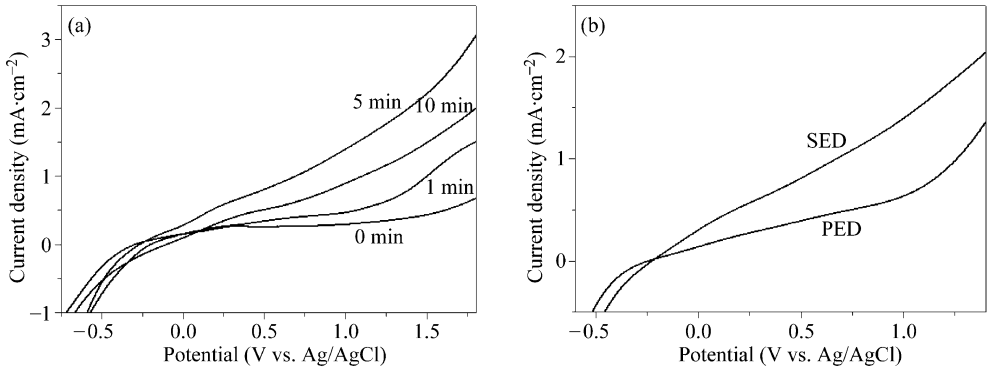

FIG. 5. (a) Photocurrent density of STNA electrode before and after Cu_2O sonoelectrochemical deposition for different periods as a function of measured potential (vs. Ag/AgCl) in 0.1 M Na_2SO_4 electrolyte solution under AM1.5 irradiation; (b) Comparison of the Photocurrent response of Cu_2O/STNA electrodes prepared by different deposition methods (the deposition time of Cu_2O is 5 min for each sample).

The photocurrent density generated by the Cu_2O/STNA electrodes and pure STNA electrode in 0.1 M Na_2SO_4 solution as a function of applied potential under white light illumination are shown in Fig. 5(a). Compared to the plain STNA electrode, the Cu_2O-modified STNA electrodes reveal evidently enhanced visible light response. At an applied potential of 1.0 V, the photocurrent density of the composite electrode (i.e. SED time of 5 min) is more than 4.75 times as high as the value of pure STNA electrode. The enhanced photocurrent response of the composite electrode means the electron/hole pair induced by simulated solar light might split and transport more readily within the electrode material. This can be ascribed to the beneficial role of the Cu_2O particles on the STNA electrode surface in improving the band structure as well as the charge separation and transfer performance. Moreover, it is not surprising that with the deposition time of Cu_2O increased from 1 to 10 min, the atomic ratio of Cu to Ti also increased from 0.015 to 0.27 accordingly (see Fig. S2 in Supplementary Information). However, the photocurrent density of Cu_2O/STNA increases as the Cu_2O deposition time increases from 1 to 5 min and decreases with a further increase in the deposition time (10 min). This might be due to a very high Cu_2O loading, which reduces the reactivity contributed by the TiO_2 nanotubes and Cu_2O particles inside the tubular structure, ultimately decreasing the overall photoactivity of the nanocomposite electrode material.

In order to examine the effect of ultrasonic waves, Figure 5(b) depicts the variation of photocurrent response in 0.1 M Na_2SO_4 for Cu_2O/STNA electrodes prepared using SED and PED, respectively. The composite electrode obtained by SED obviously shows an obvious enhanced photocurrent density compare to that fabricated by PED. At an applied potential of 1.0 V (vs. Ag/AgCl), the photocurrent density of the former electrode is ~2.2 times as high as that of the latter. The reasons responsible for the enhancement remain unclear at present. This is a subject of current research in our laboratory. We believe that many factors including the Cu_2O deposition method as well as the density and the size of loaded Cu_2O particles influence the photoelectrochemical performance of the composite electrode material. Further information about the contribution of the UV and visible components of the solar spectrum was calculated by

doing one experiment under AM 1.5 conditions and one more using an optical filter. The current density obtained under the former condition was attributed to the contribution of both UV and visible part of the solar spectrum, while the current density obtained under the latter condition was only from the contribution of visible light. As can be seen from Fig. 6, ~72.20% of the photoactivity of Cu_2O/STNA is contributed by the visible components, whereas for the pure STNA electrode, majority of their reactivity in the UV region contributes to the rest of the photoactivity (98.94%).

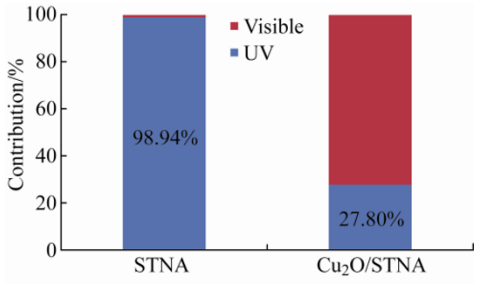

FIG. 6. Contribution of UV and visible component of the solar spectrum to the overall reactivity of the Cu_2O/STNA electrode and pure STNA electrode.

The stability of the composite electrode was examined by potentiostatic (current vs. time, I-t) measurements. Figure 7 shows the I-t curves obtained from the Cu_2O/STNA electrode at two different bias potentials under visible-light illumination. Upon switching off the light, the photocurrent density goes down to zero; whereas the photocurrent increases rapidly to the original value when under illumination again. This indicates that the current observed for this system is mainly due to the photoreactivity of the catalyst and the charge transfer within the composite electrode is very fast. Moreover, composite electrode exhibits excellent reproducibility of the I-t curves.

Conclusions

In conclusion, surface modification of STNA using facile sonoelectrochemical technique can successfully fabricate an efficient Cu_2O/STNA photoelectrode for photoelectrochemical applications. This electrode material has coupled the advantages of the chemical stability and excellent charge separation and transfer properties of STNA electrode, the photon absorbance spectrum of Cu_2O as well as the sonication technology to form n-TiO_2/P-Cu_2O heterostructure composite electrode. Experimental results have demonstrated that the presence of Cu_2O significantly extends the response of TiO_2 nanotubes into the visible region. Moreover, the enhanced photoelectrochemical properties and mechanical stability of the composite electrode material make it a highly efficient photoanode material for various potential applications.

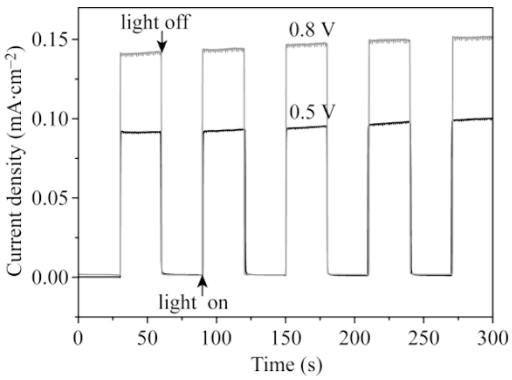

FIG. 7. Photocurrent response of a Cu_2O/STNA composite electrode biased at 0.5 V (vs. Ag/AgCl) and 0.8 V (vs. Ag/AgCl) under visible-light illumination.

The authors would like to acknowledge the State Key Development Program for Basic Research of China (Grant No. 2009CB220004), the Shanghai Basic Research Key Project (08JC1411300, 0952nm01800), the National High Technology Research and Development Program of China (Grant No. 2009 AA063003), and Shanghai Tongji Gao Tingyao Environmental Science and Technology Development Foundation for financial support.

Received 30 November 2010; accepted 24 December; published online 8 January 2011.

References

1. A. Fujishima and K. Honda, Nature 238, 37 (1972). doi:10.1038/238037a0
2. S. U. M. Khan, M. Al-Shahry and W. B. Ingler Jr., Science 297, 2243 (2002). doi:10.1126/science.1075035
3. B. O'Regan and M. Gratzel, Nature 353, 737 (1991). doi:10.1038/353737a0
4. J. H. Park, S. Kim and A. J. Bard, Nano Lett. 6, 24 (2006). doi:10.1021/nl051807y
5. H. Kisch, S. Sakthivel, M. Janczarek and D. Mitoraj, J. Phys. Chem. C 111, 11445 (2007). doi:10.1021/jp066457y
6. S. G. Chen, M. Paulose, C. M. Ruan, G. K. Mor, O. K. Varghese, D. Kouzoudis and C. A. Grimes, J. Photochem. Photobiol. A: Chem. 177, 177 (2006). doi:10.1016/j.jphotochem.2005.05.023
7. A. A. Ismail, Appl. Catal. B: Environ. 58, 115 (2005). doi:10.1016/j.apcatb.2004.11.022
8. J. Y. Kim, S. B. Choi, J. H. Noh, S. HunYoon, S. Lee, T. H. Noh, A. J. Frank and K. S. Hong, Langmuir 25, 5348 (2009). doi:10.1021/la804310z

9. P. E. de Jongh, D. Vanmaekelbergh and J. J. Kelly, J. Electrochemi. Soc. 147, 486 (2000).
10. G. K. Mor, O. K. Varghese, R. H. T. Wilke, S. Sharma, K. Shankar, T. J. Latempa, K. S. Choi and C. A. Grimes, Nano Lett. 8, 1906 (2008). doi:10.1021/nl080572y
11. J. Herion, E. A. Niekisch and G. Scharl, Sol. Energy Mater. Sol. Cells 4, 101 (1980). doi:10.1016/0165-1633(80)90022-2
12. W. Siripala, A. Ivanovskaya, T. F. Jaramillo, S. H. Baeck and E.W. Mcfarland, Sol. Energy Mater. Sol. Cells 77, 229 (2003). doi:10.1016/S0927-0248(02)00343-4
13. N. Helaili, Y. Bessekhouad, A. Bouguelia and M. Trari, J. Hazard. Mater. 168, 484 (2009). doi:10.1016/j.jhazmat.2009.02.066
14. Y. G. Zhang, L. L. Ma, J. L. Li and Y. Yu, Environ. Sci. Technol. 41, 6264 (2007). doi:10.1021/es070345i
15. D. W. Gong, C. A. Grimes, O. K. Varghese, W. C. Hu, R. S. Singh, Z. Chen and E. C. Dickey, J. Mater. Res. 16, 3331 (2001). doi:10.1557/JMR.2001.0457
16. Y. Hou, X. Y. Li, X. J. Zou, X. Quan and G. H. Chen, Environ. Sci. Technol. 43, 858 (2009). doi:10.1021/es802420u
17. L. Huang, S. Zhang, F. Peng, H. Wang, H. Yu, J. Yang, S. Zhang, H. Zhao, Scripta Mater. 63, 159 (2010). doi:10.1016/j.scriptamat.2010.03.042
18. Z. Y. Liu, X. T. Zhang, S. Nishimoto, M. Jin, D. A. Tryk, T. Murakami and A. Fujishima, J. Phys. Chem. C 112, 253 (2008). doi:10.1021/jp0772732
19. J. L. Zhang, B. X. Zhou, Q. Zheng, J. H. Li, J. Bai, Y. B. Liu and W. M. Cai, Water Res. 43, 1986 (2009). doi:10.1016/j.watres.2009.01.035
20. Y. B. Liu, B. X. Zhou, X. J. Gan, J. H. Li, J. Bai and W. M. Cai, Appl. Catal. B: Environ. 92, 326 (2009). doi:10.1016/j.apcatb.2009.08.011
21. J. Bai, B. X. Zhou, L. H. Li, Y. B. Liu, Q. Zheng, X. Y. Zhu, W. M. Cai, J. S. Liao and L. X. Zou, J. Mater. Sci. 43, 1880 (2008). doi:10.1007/s10853-007-2418-8
22. A. O. Musa, T. Akomolafe and M. J. Carter, Sol. Energy Mater. Sol. Cells 51, 305 (1998). doi:10.1016/S0927-0248(97)00233-X
23. Y. W. Tang, Z. G. Chen, Z. J. Jia, L. S. Zhang and J. L. Li, Mater. Lett. 59, 434 (2005). doi:10.1016/j.matlet.2004.09.040
24. Q. Zheng, B. X. Zhou, J. Bai, L. H. Li, Z. J. Jin, J. L. Zhang, J. H. Li, Y. B. Liu, W. M. Cai and X. Y. Zhu, Adv. Mater. 20, 1044 (2008). doi:10.1002/adma.200701619
25. J. Bai, J. H. Li, Y. B. Liu, B. X. Zhou and W. M. Cai, Appl. Catal. B Environ. 95, 408 (2010). doi:10.1016/j.apcatb.2010.01.020
26. Y. B. Liu, B. X. Zhou, J. Bai, J. H. Li, J. L. Zhang, Q. Zheng, X. Y. Zhu and W. M. Cai, Appl. Catal. B Environ. 89, 142 (2009). doi:10.1016/j.apcatb.2008.11.034
27. Y. Hou, X. Y. Li, Q. Zhao, X. Quan and G. H. Chen, Appl. Phys. Lett. 95, 093108 (2009). doi:10.1063 /1.3224181

Supplementary Information for Enhanced Photoelectrochemical Properties of Cu_2O-loaded Short TiO_2 Nanotube Array Electrode Prepared by Sonoelectro- chemical Deposition

Yanbiao Liu, Haibin Zhou, Jinhua Li, Hongchong Chen, Di Li, Baoxue Zhou*, and Weimin Cai

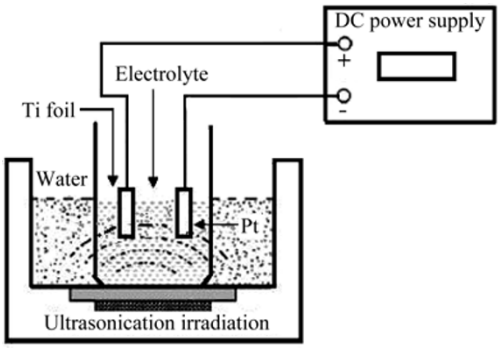

FIG. **S1.** Schematic diagram of experimental setup for anodization of Ti under ultrasonic wave irradiation.

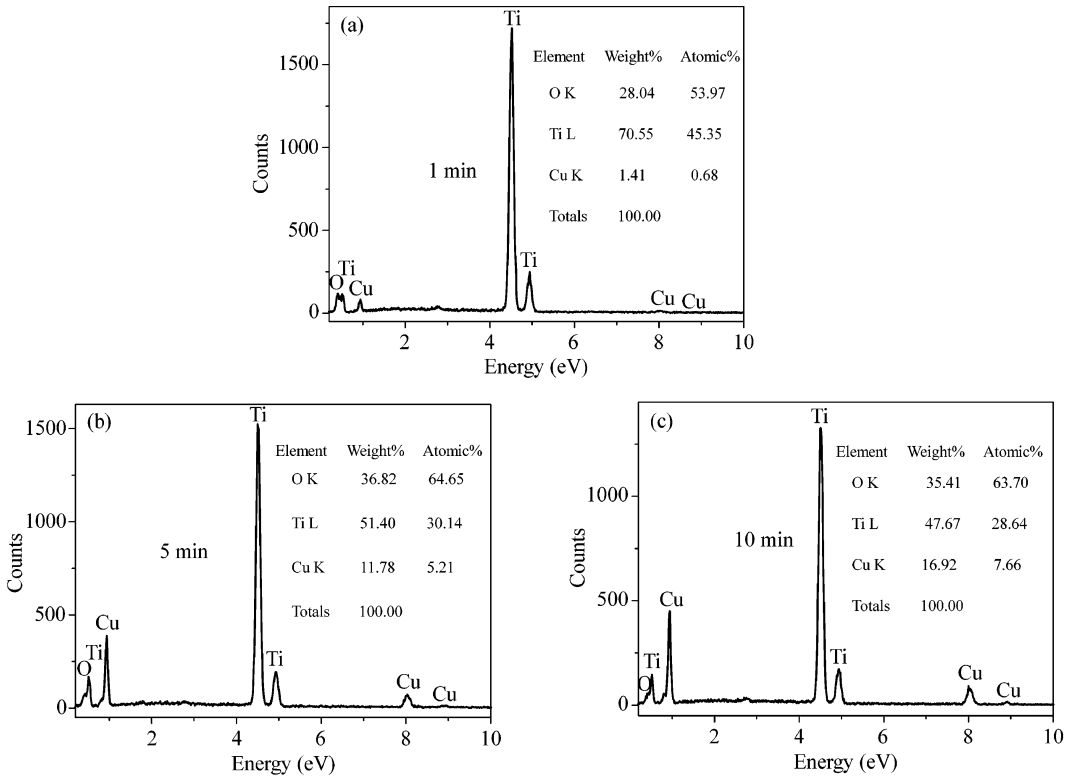

FIG. **S2**. EDX spectrum and elemental composition of the Cu_2O/STNA sample with different sonoelectrochemical deposition time of Cu_2O: (a) 1 min, (b) 5 min and (c) 10 min.